Anal Bioanal Chem (2016) 408:7155–7163
DOI 10.1007/s00216-016-9655-0

RESEARCH PAPER

Electrochemiluminescence behavior of *meso*-tetra (4-sulfonatophenyl)porphyrin in aqueous medium: its application for highly selective sensing of nanomolar Cu^{2+}

Jing Zhang[1] · **Samrat Devaramani**[1] · **Duoliang Shan**[1] · **Xiaoquan Lu**[1]

Received: 18 March 2016 / Revised: 6 May 2016 / Accepted: 18 May 2016 / Published online: 17 June 2016

Abstract The cathodic electrochemiluminescence (ECL) behavior of *meso*-tetra(4-sulfonatophenyl)porphyrin (TSPP) with potassium peroxydisulfate ($K_2S_2O_8$) as the coreactant in aqueous solution with strong and stable emission was exploited to determine Cu^{2+} down to nanomolar concentration. Two possible reaction mechanisms have been proposed to understand the generation of ECL by the TSPP/$K_2S_2O_8$ system. The effects of the concentration of TSPP and $K_2S_2O_8$, pH of the medium, and scan rate on the ECL intensity were studied in detail. The ECL intensity was efficiently quenched by trace amounts of Cu^{2+}. This phenomenon was used to develop a new method, which can offer rapid, reliable, and selective detection of Cu^{2+}. Under the optimum conditions, plots of the ECL of the TSPP/$K_2S_2O_8$ system versus the concentration of Cu^{2+} are linear in the range of 5 to 160 nM with a detection limit of 1.56 nM (S/N = 3). The proposed ECL sensor was successfully applied for analysis of tap and river water samples. It is anticipated that TSPP could be a new class of promising luminescent agent for ECL sensors.

Keywords TSPP · $K_2S_2O_8$ · Electrochemiluminescence · Cu^{2+} · Sensor

Published in the topical collection *Analytical Electrochemiluminescence* with guest editors Hua Cui, Francesco Paolucci, Neso Sojic, and Guobao Xu.

Electronic supplementary material The online version of this article (doi:10.1007/s00216-016-9655-0) contains supplementary material, which is available to authorized users.

✉ Xiaoquan Lu
Taaluxq@126.com; luxq@nwnu.edu.cn

[1] Key Laboratory of Bioelectrochemistry & Environmental Analysis of Gansu Province, College of Chemistry & Chemical Engineering, Northwest Normal University, Lanzhou, Gansu 730070, China

Introduction

Electrochemiluminescence (ECL) is the process in which electrogenerated reactive species at working electrodes undergo high energy electron transfer reactions to form excited states that emit luminescent signals [1, 2]. As an analytical technique, ECL is a promising tool that is capable of sensing and detecting a wide variety of samples as a result of the chemiluminescent analysis (low background optical signal) and the electrochemical analysis (controlled electrochemical potential) [3]. ECL has advantages over conventional electrochemical methods such as high sensitivity, wide dynamic response concentration range, and simple instrumentation [4–6]. ECL has been utilized for the determination of a wide variety of analytes from different background including medical diagnostics [7, 8], food [9, 10], water [11], and the immune system [12]. There are several classic ECL luminophores such as tris(2,2-bipyridyl)ruthenium(II) ($Ru(bpy)_3^{2+}$), luminol, lucigenin, 9,10-diphenylanthracene (DPA), peroxide oxalate, and quantum dots. Efforts have continued to develop ECL systems based on new luminescent materials. However, ECL systems based on water-soluble porphyrin as the luminophore are rare [13].

Porphyrins are a special kind of organic compound in nature as they play an important role in biological systems [14, 15]. There are many porphyrins and their metal complexes, such as heme, chlorophyll, vitamin B_{12}, cytochrome P-450, and catalase. Electrochemical and photochemical properties of porphyrins have been of interest for a long time because of their important roles in biological processes such as photosynthesis, oxygen transport, and biocatalysis [16–18]. Porphyrins are also potentially useful in the field of photomedicine, energy conversion, and catalysis [19–21]. Naturally occurring porphyrin

compounds are water soluble and have special physiological activity. People use synthetic porphyrins to simulate the properties of the natural porphyrin compounds [22]; research on water-soluble porphyrins is of particular importance.

The ECL of porphyrins was first reported by Bard et al. They reported that the ECL behavior of metalloporphyrins M(TPP) in methylene chloride (CH_2Cl_2) solution containing 0.1 M tetra-*n*-butylammonium perchlorate (TBAP) was generated via annihilation [23, 24]. Vogler's group [25] observed ECL of the tetrakis(diphosphonato)diplatinate(II) (PtTPP) using annihilation methodology. Bolin and Richter illustrated the anodic ECL of 5,10,15,20-tetraphenyl-21*H*, 23*H*-porphyrin ruthenium(II) carbonyl [Ru(TPP)(CO)] in the presence of tri-*n*-propylamine (TPrA) as a coreactant in acetonitrile [26]. However, these experiments were carried out in organic solvents. The ECL behavior of different porphyrin derivatives and complexes has been studied and used for the sensing of various analytes. In most cases, either a porphyrin derivative or complex was fixed on the electrode surface [27–29] or organic solvent was used to carry out the electrochemical experiments [30]. The ECL behavior of *meso*-tetra(4-carboxyphenyl)porphyrin (TCPP) in an aqueous medium was explored by our group and it has been used for quantifying pheophorbide in spinach samples [31].

Copper is an essential trace element which plays very important role in humans and other animals [32]. Copper is a widely used metal ion in industry, and its potential applications in chemistry, biomedicine, and environmental studies are well known [33]. Because of excessive use and improper treatment of industrial effluents, copper is a common pollutants. Bioaccumulation of copper results in several diseases such as Wilson's disease, Menkes syndrome, Alzheimer's disease, and amyotrophic lateral sclerosis [34].

It is always more convenient and easy to carry out electrochemical experiments in an aqueous medium rather than organic solvents. The ECL behavior of TSPP, a water-soluble porphyrin, has not been reported. Hence, in this work, we demonstrate the cathodic ECL behavior of the TSPP system containing $K_2S_2O_8$ as a coreactant in aqueous solution, and the possible ECL mechanisms are proposed. The electroreduced TSPP can readily react with a coreactant to produce an excited state which subsequently decays back to its ground state by emitting strong luminescence. Factors affecting the ECL response were studied carefully and optimized. The ECL signal of the TSPP/$K_2S_2O_8$ system was significantly quenched by Cu^{2+}. A highly sensitive and selective ECL method was therefore developed for the sensing of Cu^{2+} based on its interaction with the TSPP/$K_2S_2O_8$ system. The findings open new avenues to construct ECL analytical systems based on TSPP as it is stable and cost-effective.

Materials and methods

Chemicals

All chemicals and reagents were of analytical grade and used as received without further purification. *meso*-Tetra(4-sulfonatophenyl)porphyrin (TSPP) (Fig. S1 Electronic Supplementary Material, ESM) was synthesized according to the reported method [35, 36]. $K_2S_2O_8$ was obtained from Shuangshuang Chemical Co. (Yantai, China). $CuSO_4$ was purchased from Shanghai Chemical Reagent Co. K_2HPO_4, KH_2PO_4, and KCl were obtained from Zhengzhou Tianzhihao Co. The 0.1 mol/L phosphate buffer (PB) was prepared by mixing 0.1 mol/L potassium dihydrogen phosphate (KH_2PO_4) with 0.1 mol/L dipotassium hydrogen phosphate (K_2HPO_4) containing 0.1 mol/L KCl as a supporting electrolyte. The pH of the buffer was adjusted to the desired value using potassium hydroxide (KOH) and phosphoric acid (H_3PO_4). Doubly distilled water was used throughout the experiments.

Apparatus

Cyclic voltammetry (CV) and ECL experiments were carried out on an MPI-A ECL detection system (Xi' an Remex Analytical Instrument, China) equipped with a homemade ECL cell mentioned elsewhere [37]. A three-electrode system comprising a glassy carbon electrode (3 mm diameter, GCE) as working electrode, Pt counter electrode, and Ag/AgCl (saturated KCl) reference electrode was used to conduct electrochemical experiments. The voltage of the photomultiplier tube (PMT) was biased at 800 V during the whole process. Photoluminescence (PL) spectra measurements were performed on an LS-55 fluorescence spectrophotometer (Perkin Elmer). UV–vis absorption spectra were recorded on a UV-1102 UV–vis spectrophotometer (Tianmei Scientific Instrument, Shanghai, China). Infrared spectra were recorded on a Fourier transform infrared spectrometer (PTIR, NEXUS870, Nicolet Instrument Co. USA). The pHs of the solutions were measured using a Sartorius pH meter PB-10 (RenHe Instrument Co., Shanghai, China). An RE3000 rotary evaporation instrument (Shanghai, China) was used in the synthesis of TSPP.

Method

Prior to ECL measurements, the GCE was polished to a mirror finish successively with 0.3-μm and 0.05-μm α-Al_2O_3 powder on silk cloth. After each polish, the electrode was sonicated in doubly distilled water, ethanol, and distilled water then dried under nitrogen atmosphere. In this study, 0.1 M

pH 7.4 PB was always employed as the supporting electrolyte. TSPP was dissolved in ultrapure water to prepare 2.0×10^{-5} M stock solution and stored at 4 °C.

ECL measurement

Typically, the ECL experiments were performed in 0.1 M PB (pH 7.4) containing 0.1 M KCl. Firstly, TSPP (100 μL of 2.0×10^{-5} M) and $K_2S_2O_8$ (100 μL of 0.1 M) were added to a plastic tube, then they were diluted to 1000 μL with 0.1 M PBS. A 500-μL aliquot of the mixture was transferred to the ECL cell. A cyclic voltammetry (CV) scan was performed between the potential −0.3 V and −1.5 V at 100 mV s^{-1} scan rate to record the ECL signal.

ECL sensing of Cu^{2+}

The aforementioned ECL measurement procedure was adopted for Cu^{2+} sensing. A known concentration of Cu^{2+} was added to the 500 μL mixture before running the CV to record the ECL response. The standard addition method was used to record the calibration curve.

Results and discussion

The synthesized TSPP was characterized by infrared spectroscopy using the KBr pellet method. The following signal assignments were made from the obtained IR spectrum (ESM Fig. S2): The absorption peak at 3447 cm^{-1} was due to porphine ring N–H stretching vibration. Peaks at 1635 and 1472 cm^{-1} were assigned to the benzene ring and the porphyrin backbone C=C stretching vibration. Peaks at 1190, 1126, 1040, and 638 cm^{-1} are due to SO_3H group absorptions. Porphyrin ring C–H bending vibration resulted in the absorption peak at 1013 cm^{-1}. The peak at 800 cm^{-1} was due to the phenyl ring C–H bending vibration. IR and ^1H NMR (not shown) characteristics of the synthesized TSPP were found to be in good agreement with those of previous reports [35–38]. Meanwhile, the PL spectrum of TSPP with the maximum emission wavelength at 413 nm was recorded as shown in ESM Fig. S3.

To verify whether reaction occurred between TSPP and $K_2S_2O_8$ without electrolysis, UV–visible absorption spectra of the system prior to electrolysis were studied as shown in Fig. 1. The absorption spectrum of the TSPP/$K_2S_2O_8$ system was exactly the sum of the individual spectra, which implied that $K_2S_2O_8$ did not react with TSPP. Hence this showed that there is no chemical reaction between TSPP and $K_2S_2O_8$ in the ground state [39].

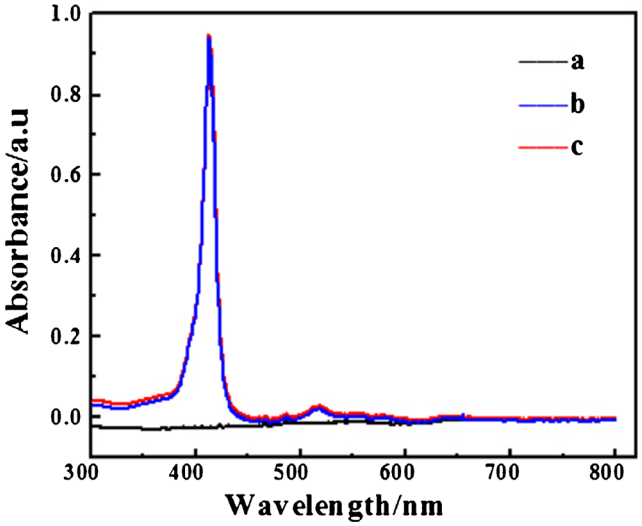

Fig. 1 UV–visible absorption spectra of *a* $K_2S_2O_8$, *b* TSPP, *c* $K_2S_2O_8$+TSPP in 0.1 mol L^{-1} PB of pH 7.4

CV and ECL behavior of TSPP

Cyclic voltammograms were recorded for the TSPP, $K_2S_2O_8$, and mixture of these two as shown in Fig. 2. For TSPP a very weak cathodic peak was observed at −0.7 V. The cathodic peak at −1.0 V was due to the electrochemical reduction of $K_2S_2O_8$ [6]. For the mixture of TSPP and $K_2S_2O_8$, the peak potential of $K_2S_2O_8$ was shifted to −1.2 V, while the cathodic peak potential of TSPP was unaltered. This indicates that TSPP hinders the $K_2S_2O_8$ electrochemical reduction under the given conditions on the GC electrode.

To understand the ECL behavior of the TSPP/$K_2S_2O_8$ system, potential was swept in the presence of only TSPP or $K_2S_2O_8$ and both TSPP and $K_2S_2O_8$. No ECL signal was observed when either TSPP or $K_2S_2O_8$ alone was present in the cell. But, mixture of TSPP and $K_2S_2O_8$ resulted in strong

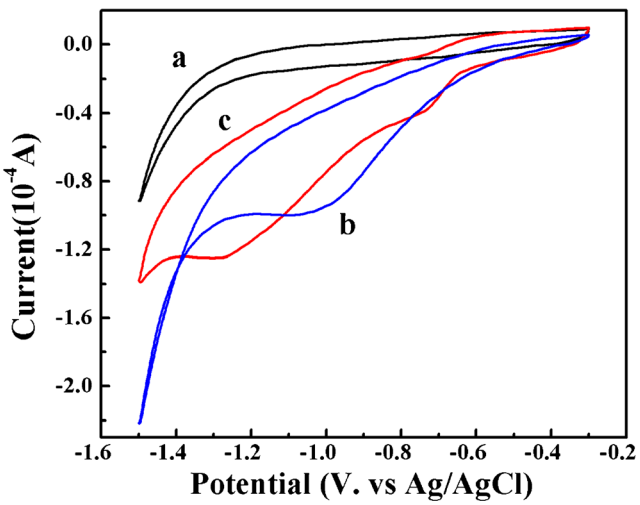

Fig. 2 Cyclic voltammograms of *a* TSPP, *b* $K_2S_2O_8$, *c* $K_2S_2O_8$+TSPP on bare glassy carbon electrode in 0.1 mol L^{-1} PB of pH 7.4

ECL signal as shown in Fig. 3. Hence, from the obtained results, it was clear that a significant ECL signal will only be observed in the presence of both TSPP and $K_2S_2O_8$.

ECL can be explained through two main mechanisms [2, 40, 41]: one is ion annihilation ECL and the other is coreactant ECL. In the present case, when the current reaches its maximum, the ECL intensity also reaches a peak value at −1.1 V. This indicates that $K_2S_2O_8$ plays an important role of coreactant in the process of generation of ECL, while TSPP act as a luminophore.

It has been reported that electrochemically oxidized or reduced porphyrins can react with coreactants to produce ECL [23–26]. The possible ECL mechanism for TSPP/$K_2S_2O_8$ is elucidated as below: when the potential was scanned from −0.3 V to −1.5 V two peaks were observed, one at about −0.7 V and the other at −1.2 V. The peak at −0.7 V was due to the electron injection from the working electrode to TSPP to produce the negatively charged species $TSPP^{\bullet-}$ (Eq. 1). Then $TSPP^{\bullet-}$ and $S_2O_8^{2-}$ interact to produce the excited state species, i.e., TSPP*, and relaxation of TSPP* to TSPP results in the ECL signal [42]:

$$TSPP + e^- \rightarrow TSPP^{\bullet-} \quad (1)$$

$$S_2O_8^{2-} + TSPP^{\bullet-} \rightarrow TSPP + SO_4^{2-} + SO_4^{\bullet-} \quad (2)$$

$$TSPP^{\bullet-} + SO_4^{\bullet-} \rightarrow SO_4^{2-} + TSPP* \quad (3)$$

$$TSPP* \rightarrow TSPP + h\upsilon \quad (4)$$

The second reduction in the ECL signal at about −1.2 V was due to reduction of $S_2O_8^{2-}$ to produce the strong oxidant species $SO_4^{\bullet-}$ (Eq. 6). Then electron transfer takes place between the produced $SO_4^{\bullet-}$ and $TSPP^{\bullet-}$, which is already present in the solution, to produce the excited state TSPP, i.e., TSPP* (Eq. 7). Then TSPP* will return to its ground state, TSPP, by emitting the ECL signal. The series of reactions which lead to the ECL signal are as follows:

$$TSPP + e^- \rightarrow TSPP^{\bullet-} \quad (5)$$

$$S_2O_8^{2-} + e^- \rightarrow SO_4^{2-} + SO_4^{\bullet-} \quad (6)$$

$$TSPP^{\bullet-} + SO_4^{\bullet-} \rightarrow SO_4^{2-} + TSPP* \quad (7)$$

$$TSPP* \rightarrow TSPP + h\upsilon \quad (8)$$

The main difference between the two mechanisms is the origin of the intermediate species $SO_4^{\bullet-}$. Because of the direct electron injection from the electrode to $S_2O_8^{2-}$, the reaction rate of Eq. 6 is greater than Eq. 2, which leads to the ECL intensity of the peak at −1.2 V being twice as high compared to the peak at −0.7 V. As discussed in the literature [43, 44], $SO_4^{\bullet-}$ has been shown to transfer electrons in the ECL reaction sequence. Scheme 1 shows the mechanism.

Another possible pathway for the generation of TSPP* is described by Eqs. 9 and 10.

$$TSPP + SO_4^{\bullet-} \rightarrow TSPP^+ + SO_4^{2-} \quad (9)$$

$$TSPP^+ + TSPP^{\bullet-} \rightarrow TSPP* + TSPP \quad (10)$$

However, the ECL versus potential trace in Fig. 3 shows little or no ECL activity prior to oxidation of both TSPP and $S_2O_8^{2-}$, indicating that light emission via Eqs. 9 and 10 is less likely to happen.

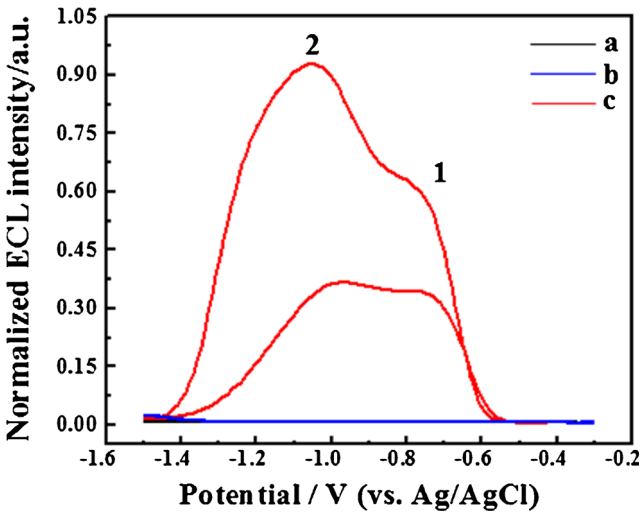

Fig. 3 ECL intensity vs. potential curves of *a* TSPP, *b* $K_2S_2O_8$, *c* $K_2S_2O_8$ + TSPP on bare glassy carbon electrode in 0.1 mol L^{-1} PB of pH 7.4. *Peaks 1* and *2* were due to the electron injection from the working electrode to TSPP and reduction of $S_2O_8^{2-}$, respectively

Optimization study

The ECL signal from the TSPP/$K_2S_2O_8$ system can be affected by several factors such as $K_2S_2O_8$ and TSPP concentration, pH value, and scan rate. Although H_2O_2 and $K_2S_2O_8$ can act as the ECL reductive–oxidative coreactants, their efficiency is quite different. As shown in Fig. S4 (ESM), TSPP exhibits

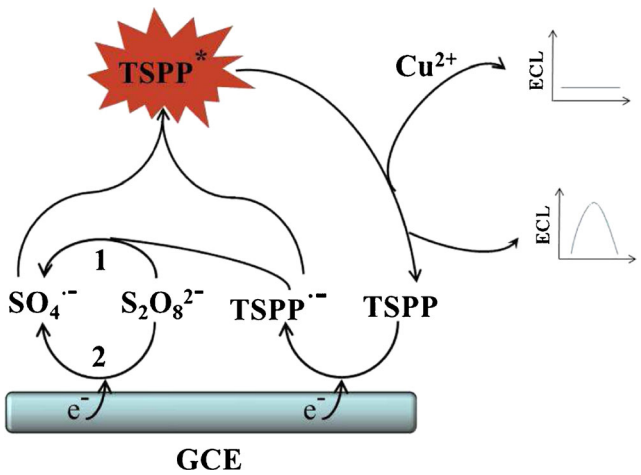

Scheme 1 ECL reaction mechanism of the TSPP/$K_2S_2O_8$ system

much stronger ECL in the presence of $K_2S_2O_8$ than in the presence of H_2O_2; therefore, $K_2S_2O_8$ was chosen as the ECL coreactant in the following experiment. Figure 4a depicts the effect of $K_2S_2O_8$ concentration on the ECL intensity. The ECL intensity increases rapidly with the increase in $K_2S_2O_8$ concentration because more TSPP* was produced from oxidation of the negatively charged TSPP by the electrogenerated $SO_4^{\bullet -}$. However, an excessive concentration of coreactants will increase the amount of reagent [45]; 0.1 M was chosen as the appropriate concentration and used throughout the following experiment. Figure 4b displays the effect of the pH of the reaction medium on the ECL intensity. The ECL intensity increases with the increase in pH from 4.5 to 7.4. Further increase in the pH resulted in the decrease of ECL signal, and the strongest ECL signal was achieved at pH 7.4, which indicated that lower alkaline conditions are suitable for TSPP ECL emission. This may be due to more active SO_3^- groups directly linked to the porphyrin ring being formed in lower alkaline conditions [46], leading to more enhanced ECL. At too high pH, the strong oxidant $SO_4^{\bullet -}$ is consumed via the scavenging effect of OH^- [47]. As a result, too low or high pH causes the decrease in the ECL intensity. Thus, pH 7.4 was chosen for this system as it would produce the stronger ECL emission. Figure 4c depicts the effect of TSPP concentration on the ECL intensity. The concentration of luminophore affects the intensity to a great extent. The ECL intensity increases with the increase of TSPP concentration and then decreased with the further increase. This can be attributed to the self-absorption effect of the luminophore [48]. As a result 2×10^{-5} mol L^{-1} of TSPP was chosen as the optimum value. ECL efficiency significantly depends on the rate of generation/annihilation of excited species. The effect of scan rate on the ECL intensity was investigated and displayed in Fig. 4d. It can be seen that the ECL intensity increases with increasing scan rate from 0.01 to 0.1 V/s and thereafter decreases. This observation was consistent with other ECL sensors. It was due to the formation a greater number of excited-state TSPP species within a short time span as well as the faster diffusion rate of the coreactant [49]. When the scan rate was higher than 0.1 V/s, the consumption of coreactant on the electrode interface would be much faster than the diffusion of the coreactant from the bulk solution to the electrode surface. Hence, it was clear that a scan rate greater than 0.1 V/s was unfavorable to the electrochemical reaction of the TSPP/$K_2S_2O_8$ system. In the following work, 0.1 V/s was selected as the optimized scan rate. The influence of different potential windows of the system on the ECL intensity was studied, and the results are shown in Fig. 4e. When the potential is too negative, hydrogen production takes place as a result of the decomposition of water and produced bubbles that can disturb the determination of the ECL. So an excitation voltage in the scanning window of −0.3 to −1.5 V was selected.

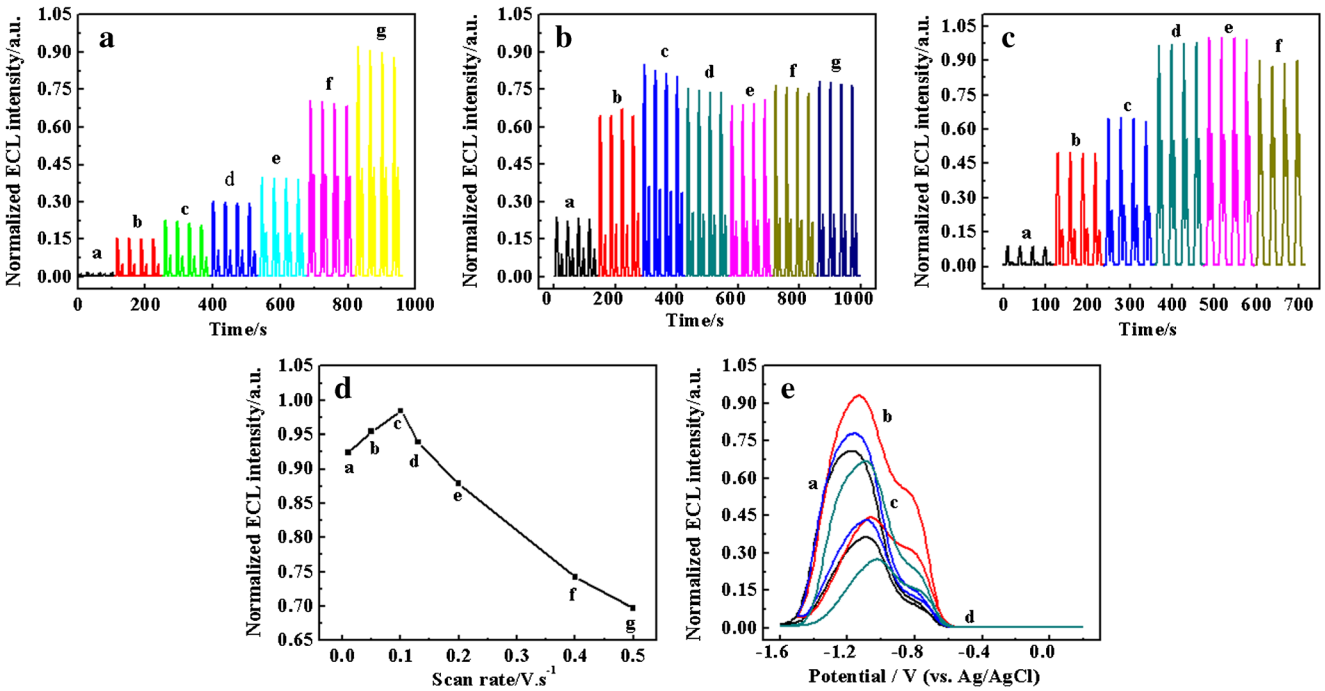

Fig. 4 Effects of (**a**) $K_2S_2O_8$ concentration ($a = 0$, $b = 0.02$, $c = 0.03$, $d = 0.04$, $e = 0.06$, $f = 0.08$, $g = 0.1$), (**b**) pH of the reaction medium ($a = 4.4$, $b = 6.4$, $c = 7.4$, $d = 8.4$, $e = 9.4$, $f = 10.4$, $g = 11.4$), (**c**) TSPP concentration ($a = 5.0 \times 10^{-6}$ M, $b = 8.0 \times 10^{-6}$ M, $c = 1.0 \times 10^{-5}$ M, $d = 1.5 \times 10^{-5}$ M, $e = 2.0 \times 10^{-5}$ M, $f = 2.5 \times 10^{-5}$ M), (**d**) scan rate ($a = 0.01$ V/s, $b = 0.05$ V/s, $c = 0.1$ V/s, $d = 0.13$ V/s, $e = 0.2$ V/s, $f = 0.4$ V/s, $g = 0.5$ V/s), and (**e**) potential window ($a = -0.3$ to -1.6 V, $b = -0.3$ to -1.5 V, $c = 0$ to -1.5 V, $d = 0.2$ to -1.6 V) on the ECL intensity of the system on bare glassy carbon electrode in 0.1 mol L^{-1} PB

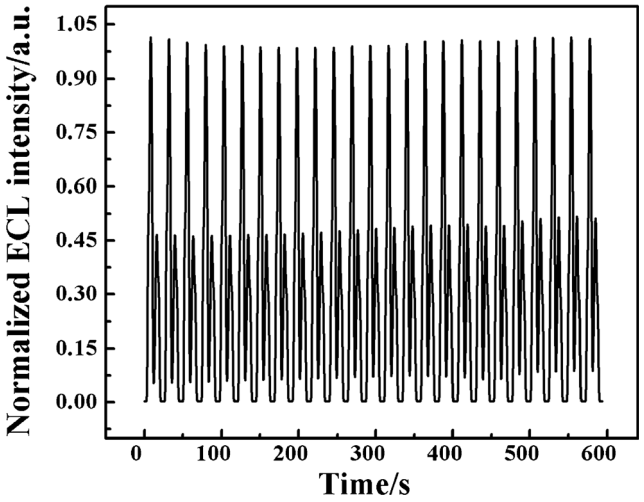

Fig. 5 ECL intensity vs. time plot for TSPP/$K_2S_2O_8$ system under optimized conditions for continuous 25 cycles

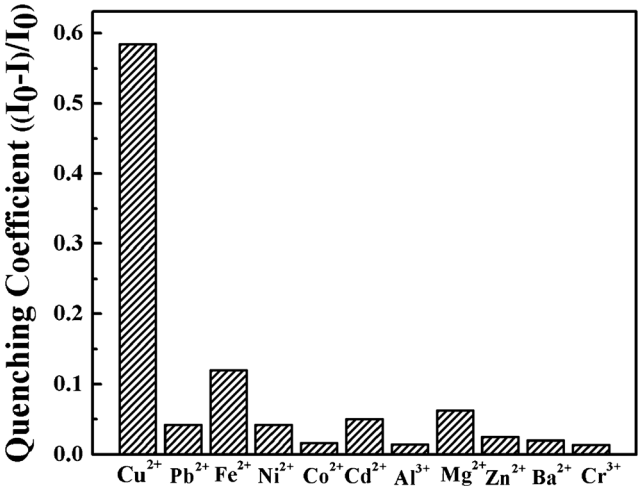

Fig. 7 Comparison of the quenching effect of various metal ions on the TSPP/$K_2S_2O_8$ system. The quenching coefficient is determined in terms of $(I_0 - I)/I_0$, where I_0 and I are the ECL intensities in the absence and presence of metal ions, respectively

Application study

Operational stability is one of the main concerns for practical application of a sensor [50]; under the optimized conditions, a stable and strong signal was exhibited by the developed system for Cu^{2+} sensing. Figure 5 shows the ECL emission of TSPP on the bare glassy carbon electrode for 25 continues cycles recorded in the potential window −0.3 to −1.5 V in 0.1 M $K_2S_2O_8$ (pH 7.4) at 0.1 V s^{-1} scan rate. The ECL signals were observed with relative standard deviation of 0.87 %. The results showed the superior stability of the ECL signal, suggesting its potential applicability as an ECL sensor.

The ECL signal response rate of the developed system to Cu^{2+} was then studied. The ECL intensity is quenched immediately as Cu^{2+} was added into the TSPP/$K_2S_2O_8$ system, and remained stable for the following 1 h as shown in ESM Fig. S5. As the quenching effect of Cu^{2+} on the ECL signal is quite fast and stable, this suggests a broad potential application to the rapid detection of Cu^{2+} with no strict time control. Figure 6 presents the quenching effect of various concentrations of Cu^{2+} on the ECL signal of the developed probe. The ECL intensity of the TSPP in the presence of Cu^{2+} (I) was lower than in the absence of Cu^{2+} (I_0), and the ECL intensity decreased gradually with the increase in Cu^{2+} concentration. Even nanomolar Cu^{2+} could effectively quench the ECL of the TSPP/$K_2S_2O_8$ system. The ECL intensity quenching and concentration of Cu^{2+} were correlated by plotting $\ln(I_0/I)$ against the added concentration of Cu^{2+}, and a linear relationship was obtained from 5 to 160 nM (Fig. 6) with a detection limit of 1.56 nM (S/N = 3) (inset Fig. 6), which is lower than or comparable to other existing ECL sensors for Cu^{2+} [51, 52]. The linear relationship can be represented as $\ln(I_0/I) = 0.0055C + 0.1967$ with a correlation coefficient of $R^2 = 0.9986$. The major characteristic of the proposed ECL sensor is that the reaction was carried out in aqueous solution, at room temperature; hence the sensor is ecofriendly and cost-effective. More importantly, it is expected that TSPP could be a new class of promising luminescent agent for ECL sensors.

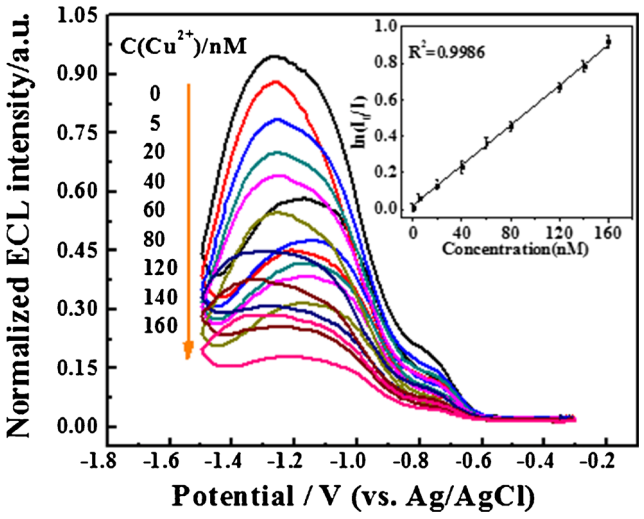

Fig. 6 ECL intensity vs. potential curves of TSPP/$K_2S_2O_8$ system under optimized conditions in the presence of various concentration of Cu^{2+}. *Inset* plot of $\ln(I_0/I)$ against the concentration of Cu^{2+}, where I_0 and I are the ECL intensities in the absence and presence of Cu^{2+}, respectively

Table 1 Determination of Cu^{2+} ion in real-life water samples

Sample	Added (nM)	Found (nM)	Recovery (%)	RSD (%, $n = 3$)
Tap water	0	Not detected		
	20	19.54 ± 0.42	97.7	6.23
	60	61.66 ± 0.26	102.7	5.54
Yellow River water	0	9.43 ± 1.21		13.45
	20	28.9 ± 1.09	98.19	6.75
	60	69.42 ± 1.53	100	3.95

In addition to sensitivity, selectivity is a very important issue when evaluating the performance of a sensing system. Hence, to assess the selectivity of the developed ECL sensor, we examined the ECL intensity changes in the presence of common metal ions as potential interfering agents. Figure 7 shows the ECL response of the TSPP/$K_2S_2O_8$ system on the bare carbon electrode in the presence of various metal ions under the optimized conditions. Only Cu^{2+} dramatically quenches the ECL intensity of the TSPP/$K_2S_2O_8$ system, whereas Pb^{2+}, Fe^{2+}, Ni^{2+}, Co^{2+}, Al^{3+}, Zn^{2+}, Mg^{2+}, Ba^{2+}, Cr^{3+}, and Cd^{2+} ions showed negligible quenching effects. The TSPP/$K_2S_2O_8$ system is therefore highly selective towards Cu^{2+} in the presence of other common metal ions. Though the reason for the selectivity of the TSPP system is not clear, the selectivity of porphyrin-based systems towards Cu^{2+} is not new [53, 54]. A probable reason for this behavior can be explained by two different mechanisms. One is that Cu^{2+} will form a covalent bond with the nitrogen atoms of pyrrole rings and dative bonds with the other nitrogen atoms of the porphyrin [55, 56]. It is well known that the photophysical properties of metalloporphyrins are entirely different from those of porphyrin; in other words, metalloporphyrins will alter the florescence of the original system [57]. Paramagnetism of the Cu^{2+} is the other possible reason that explains the selectivity. Paramagnetic Cu^{2+} may cause the reversible electron transfer in the system which may result in the quenching of fluorescence, or Cu^{2+} may cause electron spin-orbit coupling and transform the excited singlet state to a triplet state which quenches the fluorescence of the system by internal conversion [54]. Maybe any one or all the aforementioned pathways are true for the developed system, which explains both the mechanism and selectivity of the TSPP/$K_2S_2O_8$ system through which it senses Cu^{2+}.

To demonstrate the applicability of the developed Cu^{2+} sensor, the performance of the proposed method was tested to detect the concentration of Cu^{2+} in different real-life water samples obtained from Yellow River at Lan Zhou, Gansu province, China and tap water from our laboratory. The Yellow River water samples were filtered through 0.22-μm membranes and then centrifuged at 12,000 rpm for 20 min to remove sediment and suspended solids before use [48]. The resultant water samples were further used to estimate the Cu^{2+} using the developed method. For the Yellow River water samples, experimental results showed the decrease in the ECL intensity, and its comparison with the standard calibration curve suggested the presence of Cu^{2+} ions. As shown in Table 1, the Yellow river water sample contains 9.43 ± 1.21 nM Cu^{2+}, but Cu^{2+} ions are not detected in the tap water. The average recoveries of the spiked samples were in the range of 97.7 % to 102.7 %. These results indicate that the proposed method based on ECL is efficient and applicable for real sample analysis.

Conclusion

The cathodic ECL behavior of TSPP with $K_2S_2O_8$ as the coreactant in aqueous solution was explored. An ECL signal is generated upon sweeping the potential from −0.3 V to −1.5 V. Two cathodic peaks appeared at −0.7 V and −1.2 V as a result of the reduction of TSPP and $K_2S_2O_8$, respectively. On the basis of the experimental studies undertaken, we proposed possible mechanisms. The chemical reaction between the electrochemically generated $SO_4^{\bullet-}$ and $TSPP^{\bullet-}$ will produce a highly excited species, i.e., TSPP*, which will return to its ground state by emitting its excess energy in the form of an ECL signal. The ECL quenching property of Cu^{2+} was explored and used to develop a highly sensitive and selective method. A possible mechanism for the quenching and selectivity of the system towards Cu^{2+} has been explained. The developed method was found to be applicable for the analysis of Cu^{2+} in tap and river water samples.

Acknowledgments This work was supported by the Natural Science Foundation of China (grant nos. 21575115, 21327005, 21175108); the Program for Chang Jiang Scholars and Innovative Research Team, Ministry of Education, China (grant no. IRT1283); the Program for Innovative Research Group of Gansu Province, China (grant no. 1210RJIA001).

Compliance with ethical standards

Conflict of interest The authors declare that they have no competing interests.

References

1. Bard AJ. Electrogenerated chemiluminescence. New York: Dekker; 2004.
2. Richter MM. Electrochemiluminescence (ECL). Chem Rev. 2004;104(6):3003–36.
3. Dini D. Electrochemiluminescence from organic emitters. Chem Mater. 2005;17(8):1933–45.
4. Yin XB, Dong S, Wang E. Analytical applications of the electrochemiluminescence of tris(2,2′-bipyridyl)ruthenium and its derivatives. TrAC Trends Anal Chem. 2004;23(6):432–41.
5. Gerardi RD, Barnett NW, Lewis SW. Analytical applications of tris(2,2′-bipyridyl)ruthenium (III) as a chemiluminescent reagent. Anal Chim Acta. 1999;378(1):1–41.
6. Miao W. Electrogenerated chemiluminescence and its biorelated applications. Chem Rev. 2008;108(7):2506–53.
7. Bertolino C, MacSweeney M, Tobin J, et al. A monolithic silicon based integrated signal generation and detection system for monitoring DNA hybridisation. Biosens Bioelectron. 2005;21(4):565–73.
8. Ding C, Ge Y, Zhang S. Electrochemical and electrochemiluminescence determination of cancer cells based on aptamers and magnetic beads. Chem Eur J. 2010;16(35):10707–14.
9. Rivera VR, Gamez FJ, Keener WK, et al. Rapid detection of Clostridium botulinum toxins A, B, E, and F in clinical samples, selected food matrices, and buffer using paramagnetic bead-based

electrochemiluminescence detection. Anal Biochem. 2006;353(2): 248–56.
10. Huang B, Zhou X, Xue Z, et al. Quenching of the electrochemiluminescence of $Ru(bpy)_3^{2+}$/TPA by malachite green and crystal violet. Talanta. 2013;106:174–80.
11. Zhang M, Ge L, Ge S, et al. Three-dimensional paper-based electrochemiluminescence device for simultaneous detection of Pb^{2+} and Hg^{2+} based on potential-control technique. Biosens Bioelectron. 2013;41:544–50.
12. Su Q, Xing D, Zhou X. Magnetic beads based rolling circle amplification- electrochemiluminescence assay for highly sensitive detection of point mutation. Biosens Bioelectron. 2010;25(7): 1615–21.
13. Chen FC, Ho JH, Chen CY, et al. Electrogenerated chemiluminescence of sterically hindered porphyrins in aqueous media. J Electroanal Chem. 2001;499(1):17–23.
14. Venkataramanan NS, Kuppuraj G, Rajagopal S. Metal–salen complexes as efficient catalysts for the oxygenation of heteroatom containing organic compounds—synthetic and mechanistic aspects. Coord Chem Rev. 2005;249(11):1249–68.
15. Dunbar ADF, Brittle S, Richardson TH, et al. Detection of volatile organic compounds using porphyrin derivatives. J Phys Chem B. 2010;114(36):11697–702.
16. Brun AM, Harriman A. Energy-and electron-transfer processes involving palladium porphyrins bound to DNA. J Am Chem Soc. 1994;116(23):10383–93.
17. Wang W, Shan D, Yang Y, et al. A novel method for dynamic investigations of photoinduced electron transport using functionalized-porphyrin at ITO/liquid interface. Chem Commun. 2011;47(24):6975–7.
18. Lu X, Zhang L, Li M, et al. Electrochemical characterization of self-assembled thiol-porphyrin monolayers on gold electrodes by SECM. ChemPhysChem. 2006;7(4):854–62.
19. Aviv I, Gross Z. Iron corroles and porphyrins as very efficient and highly selective catalysts for the reactions of α-diazo esters with amines. Synlett. 2006;6:951–3.
20. Hod I, Sampson MD, Deria P, et al. Fe-porphyrin-based metal–organic framework films as high-surface concentration, heterogeneous catalysts for electrochemical reduction of CO_2. ACS Catal. 2015;5(11):6302–9.
21. Lin S, Diercks CS, Zhang YB, et al. Covalent organic frameworks comprising cobalt porphyrins for catalytic CO2 reduction in water. Science. 2015;349(6253):1208–13.
22. Constantin C, Neagu M. Fluorescent porphyrin with an increased uptake in peripheral blood cell subpopulations from colon cancer patients. Med Chem. 2015;11(4):354–63.
23. Tokel NE, Keszthelyi CP, Bard AJ. Electrogenerated chemiluminescence. X. α, β, γ, δ-Tetraphenylporphine chemiluminescence. J Am Chem Soc. 1972;94(14):4872–7.
24. Tokel-Takvoryan NE, Bard AJ. Electrogenerated chemiluminescence. XVI. ECL of palladium and platinum α, β, γ, δ-tetraphenylporphyrin complexes. Chem Phys Lett. 1974;25(2): 235–8.
25. Vogler A, Kunkely H. Electrochemiluminescence of tetrakis(diphosphonato)diplatinate(II). Angew Chem Int Ed Engl. 1984;23(4):316–7.
26. Bolin A, Richter MM. Coreactant electrogenerated chemiluminescence of ruthenium porphyrins. Inorg Chim Acta. 2009;362(6): 1974–6.
27. Wu L, Wang J, Feng L, et al. Label-free ultrasensitive detection of human telomerase activity using porphyrin-functionalized graphene and electrochemiluminescence technique. Adv Mater. 2012;24(18):2447–52.
28. Zhang GY, Deng SY, Zhang XJ, et al. Cathodic electrochemiluminescence of singlet oxygen induced by the electroactive zinc porphyrin in aqueous media. Electrochim Acta. 2016;190:64–8.
29. Xu N, Lei J, Wang Q, et al. Dendritic DNA–porphyrin as mimetic enzyme for amplified fluorescent detection of DNA. Talanta. 2016;150:661–5.
30. Long TR, Richter MM. Electrogenerated chemiluminescence of the platinum (II) octaethylporphyrin/tri-n-propylamine system. Inorg Chim Acta. 2005;358(6):2141–5.
31. Luo D, Huang B, Wang L, et al. Cathodic electrochemiluminescence of meso-tetra(4-carboxyphenyl)porphyrin/potassium peroxydisulfate system in aqueous media. Electrochim Acta. 2015;151:42–9.
32. Cheng C, Huang Y, Tian X, et al. Electrogenerated chemiluminescence behavior of graphite-like carbon nitride and its application in selective sensing Cu^{2+}. Anal Chem. 2012;84(11):4754–9.
33. Tian J, Liu Q, Asiri AM, et al. Ultrathin graphitic carbon nitride nanosheet: a highly efficient fluorosensor for rapid, ultrasensitive detection of Cu^{2+}. Anal Chem. 2013;85(11):5595–9.
34. Cheng N, Jiang P, Liu Q, et al. Graphitic carbon nitride nanosheets: one-step, high-yield synthesis and application for Cu^{2+} detection. Analyst. 2014;139(20):5065–8.
35. Lindsey JS, Schreiman IC, Hsu HC, et al. Rothemund and Adler-Longo reactions revisited: synthesis of tetraphenylporphyrins under equilibrium conditions. J Org Chem. 1987;52(5):827–36.
36. Lindsey JS, MacCrum KA, Tyhonas JS, et al. Investigation of a synthesis of meso-porphyrins employing high concentration conditions and an electron transport chain for aerobic oxidation. J Org Chem. 1994;59(3):579–87.
37. Lu X, Wang H, Du J, et al. Self-quenching in the electrochemiluminescence of tris(2,2′-bipyridyl) ruthenium(II) using metabolites of catecholamines as coreactants. Analyst. 2012;137(6):1416–20.
38. He Q. Effect of the local environment on the structure and reactivity of metalloporphyrins. Science: Department of Chemistry. Ph.d. Thesis. 2010.
39. Vinyard DJ, Swavey S, Richter MM. Photoluminescence and electrogenerated chemiluminescence of a bis(bipyridyl)ruthenium (II)–porphyrin complex. Inorg Chim Acta. 2007;360(5):1529–34.
40. Wang Y, Lu J, Tang L, et al. Graphene oxide amplified electrogenerated chemiluminescence of quantum dots and its selective sensing for glutathione from thiol-containing compounds. Anal Chem. 2009;81(23):9710–5.
41. Chen Y, Shen Y, Sun D, et al. Fabrication of a dispersible graphene/gold nanoclusters hybrid and its potential application in electrogenerated chemiluminescence. Chem Commun. 2011;47(42):11733–5.
42. White HS, Bard AJ. Electrogenerated chemiluminescence. 41. Electrogenerated chemiluminescence and chemiluminescence of the Ru $(2,2^1\text{-bpy})_3^{2+}$-$S_2O_8^{2-}$ system in acetonitrile-water solutions. J Am Chem Soc. 1982;104(25):6891–5.
43. Liang G, Shen L, Zou G, et al. Efficient near-infrared electrochemiluminescence from CdTe nanocrystals with low triggering potential and ultrasensitive sensing ability. Chem Eur J. 2011;17(37):10213–5.
44. Bae Y, Myung N, Bard AJ. Electrochemistry and electrogenerated chemiluminescence of CdTe nanoparticles. Nano Lett. 2004;4(6): 1153–61.
45. Yao W, Wang L, Wang H, et al. Cathodic electrochemiluminescence behavior of norfloxacin/peroxydisulfate system in purely aqueous solution. Electrochim Acta. 2008;54(2):733–7.
46. Yu S, Zhou Q, Zhao XM, et al. Comparison of the antiviral effects of different nucleos(t)ide analogues in Chinese patients with chronic hepatitis B: a head-to-head study. Saudi J Gastroenterol. 2014;20(6):350.
47. Chen Z, Wong KMC, Kwok ECH, et al. Electrogenerated chemiluminescence of platinum(II) alkynyl terpyridine complex with peroxydisulfate as coreactant. Inorg Chem. 2011;50(6):2125–32.

48. Hua L, Han H, Chen H. Enhanced electrochemiluminescence of CdTe quantum dots with carbon nanotube film and its sensing of methimazole. Electrochim Acta. 2009;54(5):1389–94.
49. Dai H, Chi Y, Wu X, et al. Biocompatible electrochemiluminescent biosensor for choline based on enzyme/titanate nanotubes/chitosan composite modified electrode. Biosens Bioelectron. 2010;25(6): 1414–9.
50. Shang Q, Zhou Z, Shen Y, et al. Potential-modulated electrochemiluminescence of carbon nitride nanosheets for dual-signal sensing of metal ions. ACS Appl Mater Interface. 2015;7(42):23672–8.
51. De Silva AP, Gunaratne HQN, Gunnlaugsson T, et al. Signaling recognition events with fluorescent sensors and switches. Chem Rev. 1997;97(5):1515–66.
52. Luo HY, Zhang XB, Jiang JH, et al. An optode sensor for Cu^{2+} with high selectivity based on porphyrin derivative appended with bipyridine. Anal Sci. 2007;23(5):551–5.
53. Ghosh I, Saleh N, Nau WM. Selective time-resolved binding of copper (II) by pyropheophorbide-a methyl ester. Photochem Photobiol Sci. 2010;9(5):649–54.
54. Hu M, Li H, Chen L, et al. Fluorescence quenching of pheophytin-a by copper (II) ions. Chin J Chem. 2009;27(3):513–7.
55. Domingues MRM, Santana-Marques MG, Ferrer-Correia AJ. Formation of metalloporphyrins and metallochlorins in the source of a mass spectrometer under fast atom bombardment. Int J Mass Spectrom Ion Process. 1997;165–166:551–9.
56. Giovannetti R, Bartocci V, Ferraro S, Gusteri M, Passamonti P. Spectrophotometric study of coproporphyrin-I complexes of copper(II) and cobalt(II). Talanta. 1995;42:1913–8.
57. Hu MB, Li HX, Chen LS, Zhang HB, Dong C. Fluorescence quenching of pheophytin-a by copper(II) ions. Chin J Chem. 2009;27:513–7.